D: Energy and sustainability
D.1. Energy and IEQ

CFD ANALYSIS OF VENTILATIVE COOLING IN A GENERIC ISOLATED BUILDING EQUIPPED WITH VENTILATION LOUVERS

Katarina Kosutova[1,*], Twan van Hooff[2], Bert Blocken[1,2] and Jan Hensen[1]

[1]Building Physics and Services, Department of the Built Environment, Eindhoven University of Technology, The Netherlands
[2]Building Physics Section, Department of Civil Engineering, Leuven University, Leuven, Belgium

[*]Corresponding email: k.kosutova@tue.nl

Keywords: CFD simulations, Air exchange efficiency, Heat removal, Ventilation louvers.

SUMMARY

This study presents Computational Fluid Dynamics (CFD) simulations of indoor airflow in order to assess the air exchange efficiency and heat removal in a naturally ventilated generic isolated building. The building has a window on both the windward and leeward facade to allow cross-ventilation. First, isothermal steady Reynolds-Averaged Navier-Stokes (RANS) CFD simulations were performed to validate the numerical model using Particle Image Velocimetry (PIV) experiments from literature. Subsequently, non-isothermal steady RANS CFD simulations were conducted to assess the velocity and temperature fields, the air exchange efficiency and the heat removal effectiveness. For both cases a grid-sensitivity analysis was conducted to limit the discretization errors. The CFD simulations were performed for wind direction perpendicular to the building facade with the window opening. Four different window configurations were considered; three with ventilation louvers with different slat angles (0°, 30° and 45°), and one without louvers. The results showed that the configurations with ventilation louvers with an slat angle of 30° and the configuration without louvers have the best performance with respect to ventilative cooling. This configuration had the highest air exchange efficiency (> 51%) and heat removal effectiveness (> 78%).

INTRODUCTION

Ventilative cooling can be a sustainable and energy-efficient solution to reduce energy consumption of the building for cooling, prevent indoor overheating and help maintaining a healthy indoor environment. Despite the simplicity of the concept – outdoor air flows through the building, removing the heat gains – ventilative cooling is still not widely applied in commercial and residential buildings. This can partly be attributed to the limited information about the complex indoor airflow patterns, possible thermal comfort issues (Kubota et al., 2009) and uncertainties involved (Finn et al., 2007; Artmann et al., 2008; Goethals et al., 2011).

Moreover, practical issues such as prevention of draught, rain penetration and burglary are important to consider when applying ventilative cooling. Special attention should be given to these issues to enable an efficient use of ventilative cooling. One of the possible solutions can be applying ventilation louvers. With their operable slats, it is possible to control the ventilation, light entry and to prevent rain penetration. Moreover, different positions of the slats can influence the ventilation flow and the ventilation flow rates.

In the present study, non-isothermal CFD simulations were carried out for a generic isolated building equipped with ventilation louvers on both window openings of the building. Three different louver slat angles were investigated: 0°, 30° and 45°. Furthermore, a building with windows without louvers was analyzed. The results of the CFD simulations are compared in terms of ventilation flow rates, air exchange efficiency, heat removal effectiveness and indoor air temperatures. This study provides some basic insights in the effect of ventilation louvers on ventilative cooling in a simple generic building.

CFD SIMULATIONS: VALIDATION STUDY

Computational domain and grid

Isothermal CFD simulations were carried out to validate the CFD model based on the wind-tunnel experiments of Karava (2008). More information on the experiments can be found in (Karava 2008). A generic isolated building with dimensions 100 x 100 x 80 mm^3 at scale 1:200 was considered. The wind direction was perpendicular to the building facade with the opening. Cross-ventilation in the building was ensured by a window with dimensions 22 x 18 mm^2 (W x H) on both the windward and leeward facade (Fig. 1a). The dimensions of the computational domain were 900 x 1540 x 480 mm^3 (W x L x H) (Fig. 1b) and were defined in accordance with the best practice guidelines by Franke et al. (2007) and Tominaga et al. (2008). The distance from the building to the lateral sides and to the top of the domain was 5H and the distance from the building to the outlet was 15H, with H the height of the building (= 80 mm). The upstream length was reduced to 3H in order to reduce the unintended streamwise gradients, for more details see (Blocken et al. 2007).

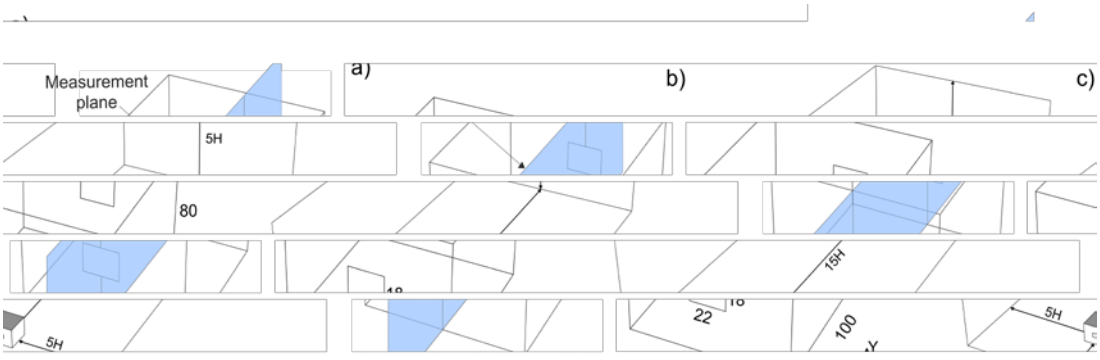

Figure 1. (a) Building geometry, (b) geometry of the computational domain (H = 80 mm), (c) perspective view indicating the measurement plane.

The structured computational grid was created using the surface extrusion technique proposed by van Hooff and Blocken (2010), which allows full control over the cell

quality. A grid-sensitivity analysis was carried out using three grids: coarse grid (350,940 cells), basic grid (1,153,876 cells) and fine grid (1,755,936 cells). Figure 2a shows the results of the grid-sensitivity analysis; streamwise velocity ratios U/U_{ref} at the centerline passing through the openings. The differences between the coarse and basic grid are very small, as well as the differences between the basic and the fine grid, which indicates nearly grid-independent results provided by the basic grid.

Boundary conditions and solver settings

A logarithmic velocity profile corresponding to the measured velocities in the wind tunnel (Karava, 2008) was imposed as an inlet boundary condition with reference velocity U_{ref} = 6.97 m/s at building height (y_{ref} = H), and an aerodynamic roughness length of y_0 = 0.025 mm. In addition, profiles for turbulent kinetic energy (k) and specific dissipation rate (ω) were defined. The turbulent kinetic energy profile was calculated based on the measured velocity and turbulence intensity using $k = (UI_U)^2$ (Ramponi and Blocken, 2012), with I_U the streamwise turbulence intensity (with a value of 10% at building height (y_{ref}) and 17% near ground level (y = 12 mm) (Karava 2008)). The specific dissipation rate ω was obtained from $\omega = \varepsilon/(C_\mu k)$, where C_μ is an empirical constant taken equal to 0.09, and the turbulence dissipation rate ε was calculated using $\varepsilon = u^*_{ABL}{}^3/(\kappa(y+y_0))$, with u^*_{ABL} the atmospheric boundary layer (ABL) friction velocity (= 0.363 m/s), κ the von Karman constant (0.42) and y the height coordinate. On the ground plane of the domain, the standard wall functions by Launder and Spalding (1974) were imposed with sand-grain based roughness modification by Cebeci and Bradshaw (1977). The values of the equivalent sand-grain roughness height k_s and the roughness constant C_s for the ground surface were determined based on the relationship with the aerodynamic roughness length y_0 derived by Blocken et al. (2007): $k_s = 9.793\, y_0/C_s$.

The 3D steady RANS equations were solved in combination with the SST k-ω turbulence model (Menter, 1994) to provide closure to the governing equations. This model emerged as the most appropriate one for the simulation of cross-ventilation in this generic isolated building (e.g. Ramponi and Blocken, 2012). Second-order discretization schemes were used for the convective and viscous terms of the governing equations and for pressure interpolation. The SIMPLE algorithm was used for the pressure-velocity coupling. Convergence was assumed to be reached when all the scaled residuals leveled off and reached minimum values 10^{-4} for continuity and specific dissipation rate and 10^{-7} for x-, y-, and z-velocity and 10^{-6} for turbulent kinetic energy.

Results

The results from the isothermal CFD simulations were compared with the PIV wind tunnel experiments by Karava (2008). The streamwise velocity ratios U/U_{ref} on the line through the center of the openings were compared (Fig. 2b). The CFD results fairly well predicted the velocities near the openings as well as the flow pattern inside of the building. The overall agreement with experimental results was fair to good, therefore the turbulence model, boundary conditions and solver settings are also used for the non-isothermal CFD simulations.

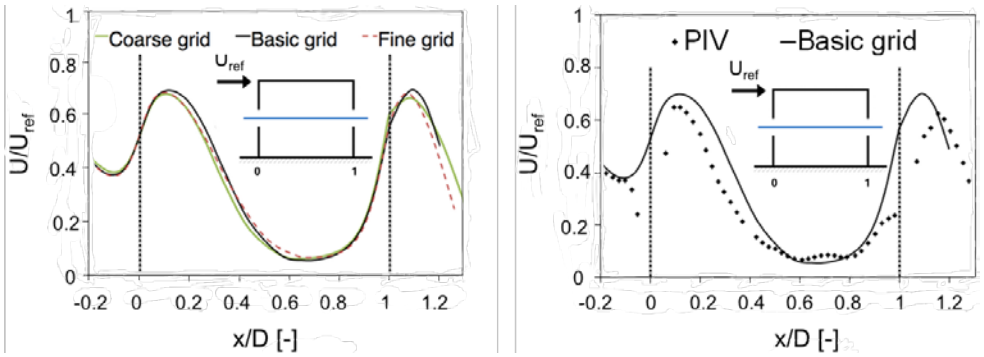

Figure 2. (a) Results of the grid-sensitivity analysis. (b) Comparison of isothermal CFD simulations using the basic grid (solid line) with PIV measurements (symbols) from Karava (2008) in terms of wind speed ratio (U/U_{ref}) along centerline.

CFD SIMULATIONS OF VENTILATIVE COOLING: COMPUTATIONAL SETTINGS AND PARAMETERS

Computational domain and grid

Full-scale non-isothermal CFD simulations were carried out to analyze the ventilative cooling for a generic isolated building at full scale, with building dimensions 5 x 5 x 4 m^3 (L x W x H) and window dimensions 1.1 x 0.9 m^2 (W x H). The dimensions of the computational domain were 77 x 45 x 24 m^3 (L x W x H). Four different computational models were made for this analysis; three models which include ventilation louvers with a slat angle of 0°, 30° and 45°(Fig. 3a-c), and one model without louvers (Fig. 3d).

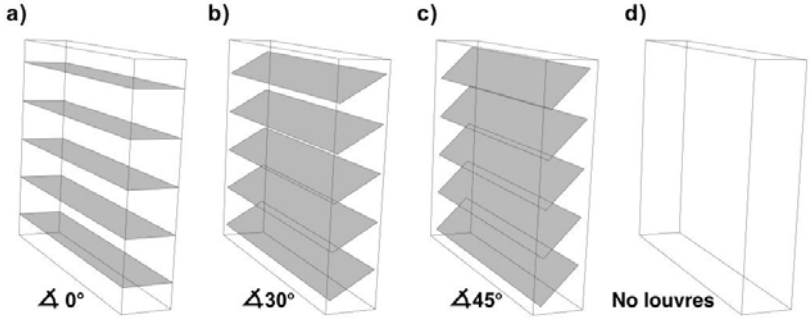

Figure 3. Window configurations studied. (a-c) Windows equipped with louvers with slat angles of: (a) 0°, (b) 30°, (c) 45°, and (d) without louvers.

A high grid resolution was applied inside the building ($y^* < 5$) to be able to resolve the flow all the way down to the wall, including the thin viscous sublayer, which is essential to obtain an accurate prediction of convective heat transfer from the interior building wall to the fluid.

A grid-sensitivity analysis was conducted in order to minimize the discretization errors. Three different grids were created by increasing the grid resolution with about an overall factor of 2: coarse grid (3,701,356), basic grid (6,766,578 cells) and fine grid (14,693,944). The results from this non-isothermal grid-sensitivity analysis were compared in terms of streamwise velocity ratio U/U_{ref} along a line through the center of the opening. The grid-sensitivity analysis indicated that nearly grid-independent results were obtained with the basic grid, which is therefore used for the analysis of the different window configurations.

Boundary conditions and solver settings

A logarithmic velocity profile was imposed at the inlet: $U(y) = (u^*_{ABL}/\kappa)\ln((y+y_0)/y_0))$ with u^*_{ABL} = 0.363 m/s, κ the von Karman constant (= 0.42) and y_0 = 0.00125 m. The profiles for k and ω were calculated using the equations for k and ω reported in the previous section. The streamwise turbulence intensity (I_U) is equal to 10% at building height (y_{ref} = 4 m) and 17% near ground level (y = 0.6 m). On the ground plane of the domain, the standard wall functions by Launder and Spalding (1974) were imposed with sand grain based roughness modification by Cebeci and Bradshaw (1977). The coefficients k_s and C_s were calculated based on $k_s = 9.793\ y_0/C_s$ (Blocken et al., 2007). The outdoor air temperature was set to 20°C, and the surface temperature of the inner surfaces of the building (including floor and ceiling) was set to 30°C to analyze the flow in the evening/night after a hot summer day.

The energy equation was enabled for the non-isothermal simulations. The turbulence model and discretization schemes were identical to those in the isothermal simulations. However, the PRESTO! algorithm was used for pressure-velocity coupling instead of the SIMPLE algorithm. Convergence was assumed to be reached when all the scaled residuals leveled off and reached minimum values 10^{-4} for continuity and specific dissipation rate, 10^{-7} for x-, y-, and z-velocity, 10^{-6} for turbulent kinetic energy, and 10^{-8} for energy. By solving an additional transport equation for a passive scalar it was possible to numerically determine the age of air inside the enclosure, and thus the air exchange efficiency (Etheridge, 2011).

RESULTS AND DISCUSSION

The ventilation flow rates and air exchange efficiencies for the four different window configurations are summarized in Figure 4. The ventilation flow rates for different louver slat angles are shown in Figure 4a. The highest ventilation flow rate is observed for a building equipped with ventilation louvers with a slat angle of 0°; 4.61 m^3/s. The volume flow rate through the window without lovers is 3.56 m^3/s, which is about 23% lower than for slat angle of 0°. The lowest volume flow rate is observed for slat angle of 45°; 2.05 m^3/s.

Figure 4b shows the air exchange efficiency, which was calculated as follows: $\varepsilon = 100\ \tau_{out}/(2\tau_{av})$, where τ_{out} is the age of air at the outlet window of the building and τ_{av} is the volume-average age of air in the room (Etheridge, 2011). The highest air exchange efficiency, 52%, is observed for the window configuration without louvers. Ventilation louvers with slat angle of 30° have an air exchange efficiency of 51%. The lowest air exchange efficiency is observed for the louvers with slat angle of 0°, which can be attributed to the short-circuiting of the flow inside the building, resulting in the absence of significant mixing inside the building (see Fig. 6c).

Figure 5a shows the heat removal effectiveness for different louver slat angles. The heat removal effectiveness is calculated using $\varepsilon_t = (\theta_e-\theta_s)/(\theta_{av}-\theta_s)$, with θ_e the average temperature at the downstream window, θ_s the average supply temperature and θ_{av} the volume-averaged temperature inside the enclosure (all in °C) (Awbi, 1998). The highest heat removal effectiveness was obtained in a building with windows without louvers: 79%. A louver slat angle of 30° results in a heat removal effectiveness of 78%. The lowest heat removal effectiveness is observed for an slat

angle of 0°: 46%. Figure 5b shows the average air temperatures inside the building, which vary from 22.2°C to 23.1°C.

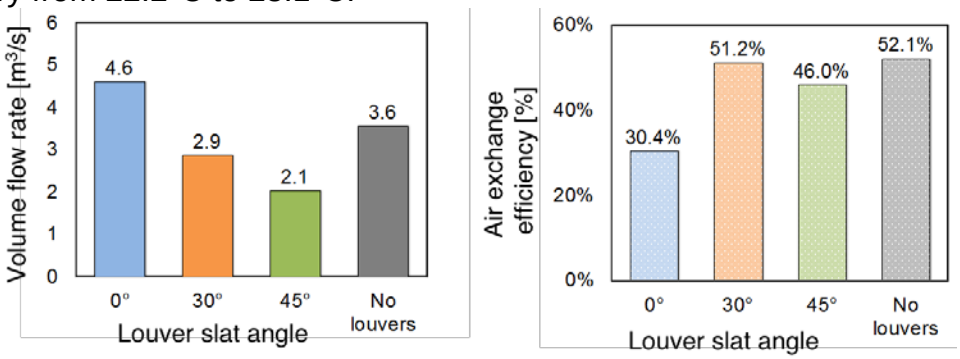

Figure 4. (a) Volume flow rates and (b) air exchange efficiency for the four different window configurations.

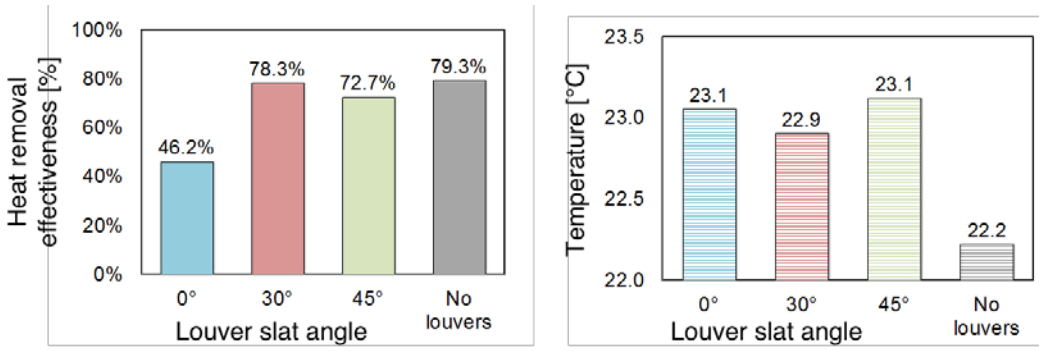

Figure 5. (a) Heat removal effectiveness; (b) average indoor temperature (θ_{ref} = 20°C) for the four different window configurations.

Figure 6 shows the contours of dimensionless velocity ($|V|/U_{ref}$) around and inside the building. It can be seen that for louver slat angles of 30° and 45° the flow is directed towards the ceiling. As a result, both configurations show a higher level of mixing of the air inside the building. Figure 6a shows that short-circuiting is present for the window configuration with an louver slat angle of 0°. Finally, Figure 6d shows that the incoming air is directed towards the floor when no ventilation louvers are present.

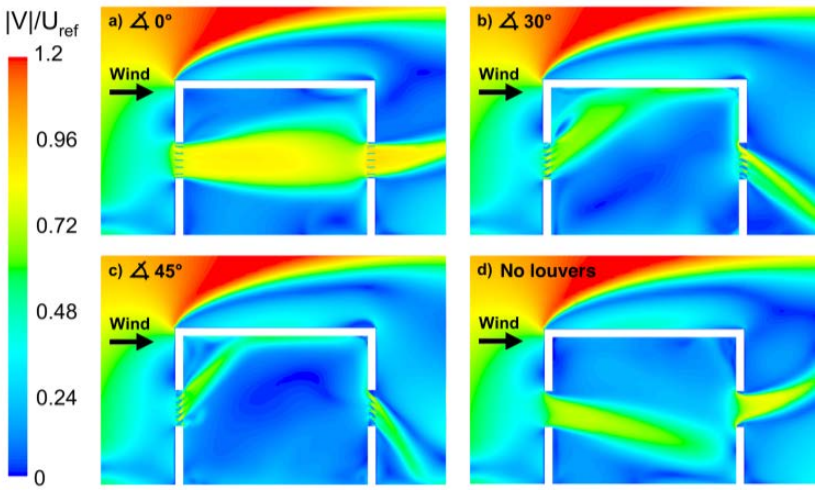

Figure 6. Contours of dimensionless velocity ($|V|/U_{ref}$) in vertical center plane obtained from the non-isothermal simulations for different louver slat angles: (a) 0°, (b) 30°, (c) 45°, and for (d) window without louvers. U_{ref} = 6.97 m/s.

Figure 7 shows the temperature distribution within the building. Due to the high reference wind speed, U_{ref} = 6.97 m/s (Ri = 0.027), the air is mainly driven by mechanical forces; the effect of buoyancy is very limited in this case. In Figure 7b and Figure 7c it can again be seen that for the configurations with slat angle of 30° and 45° the incoming cool air is directed towards the ceiling, while in Figure 7a the cool air stream flows through the center of the building in the direction of the downstream window (short-circuiting), and in Figure 7d the cold air is directed towards the floor. Figure 7d also shows that the lowest air temperatures are present in the case without ventilation louvers.

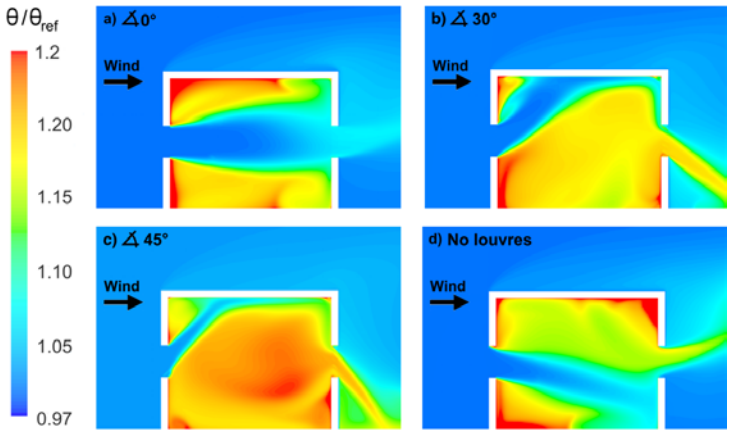

Figure 7. Contours of dimensionless temperature (θ/θ_{ref}) obtained from vertical center plane around and inside the building for different louver slat angles: (a) 0°, (b) 30°, (c) 45°, and for (d) window without louvers. θ_{ref} = 20°C.

CONCLUSIONS

This paper presented a comparative study of ventilative cooling for a generic isolated building equipped with ventilation louvers with three different louver slat angles (0°, 30° and 45°) and for windows without louvers. The results showed that different slat angles have a significant impact on the ventilation flow rates as well as on the air exchange efficiency and heat removal effectiveness. An slat angle of 0° provided the highest ventilation flow rates, however, the air exchange efficiency was the lowest of

all studied cases, resulting in a difference of 22% compared to the highest air exchange efficiency obtained for the window configuration without louvers. Furthermore, a louver slat angle of 0° resulted in the lowest heat removal effectiveness, namely 46%. Therefore, it can be concluded that a louver slat angle of 0° is the least efficient in terms of air exchange efficiency and heat removal effectiveness. The most efficient window configurations are the window configuration without louvers and the configuration with louvers with slat angle of 30°. The performance of these two configurations appeared to be very similar, except for the average indoor air temperature and volume flow rate, which are lower for the configuration without louvers.

In general, the performance is strongly related with both the airflow pattern inside the building (air exchange efficiency and heat removal effectiveness) and the supplied volume flow rate. For example, the poor performance of the configuration with an louver slat angle of 0° (which has the highest volume flow rate) can be attributed to short-circuiting of the outdoor air flow between the two windows. To optimize the ventilative cooling in a cross-ventilated building, both the volume flow rate and the airflow pattern should be optimized.

The CFD simulations in this study were carried out for a relatively high reference wind speed; therefore the flow was mainly driven by mechanical forces (Ri = 0.027). Future research will – among others – study the influence of the louver slat angle of the ventilation louvers on ventilative cooling for lower wind speeds and for higher values of the aerodynamic roughness length (e.g. y_0 = 0.5 m).

ACKNOWLEDGEMENTS

Twan van Hooff is currently a postdoctoral fellow of the Research Foundation – Flanders (FWO) and acknowledges its financial support (project FWO 12R9715N).

REFERENCES

Artmann N, Manz H, Heiselberg P (2008). Parameter study on performance of building cooling by night-time ventilation. *Renewable Energy*, **33** (12), 2589–2598.

Awbi HB (1998) Energy efficient room air distribution. *Renewable Energy*, **15**, 239-299

Blocken B, Stathopoulos T, Carmeliet J (2007). CFD simulation of the atmospheric boundary layer: wall function problems. *Atmospheric Environment*, **41**(2), 238–252.

Cebeci T, Bradshaw P (1977) *Momentum transfer in boundary layers*, Hemisphere Publishing Corporation, New York, USA

Etheridge D (2012), *Natural Ventilation of Buildings - Theory, Measurement and design*, John Wiley & Sons, Chirchester, UK

Franke J, Hellsten A, Schlünzen B et al (2007). Best practice guideline for the CFD simulation of flows in the urban environment, COST office, 2007

Goethals K, Breesch H, Janssens A (2011). Sensitivity analysis of predicted night cooling performance to internal convective heat transfer modelling. *Energy and Buildings*, **43**(9), 2429–2441.

Karava P (2008). Airflow prediction in buildings for natural ventilation design : wind tunnel measurements and simulation, PhD thesis, Department of Building, Civil and Environmental Engineering, Concordia University, Canada.

Kubota T, Chyee DTH, Ahmad S (2009). The effects of night ventilation technique on indoor thermal environment for residential buildings in hot-humid climate of Malaysia. *Energy and Buildings*, **41**(8), 829–839.

Launder BE, Spalding DB (1974). The numerical computation of turbulent flows, *Comput. Methods. Appl. Mech. Eng*., **3**, 269–289

Menter FR (1994) Two-equation eddy viscosity turbulence models for engineering applications, *AIAAJ*, **32**, 1598-1605

Ramponi R, Blocken B (2012). CFD simulation of cross-ventilation for a generic isolated building: Impact of computational parameters. *Building and Environment*, **53**, 34–48.

Tominaga Y, Mochida A, Yoshie R et al (2008). AIJ guidelines for practical applications of CFD to pedestrian wind environment around buildings. *Journal of Wind Engineering and Industrial Aerodynamics*, **96**(10-11), 1749–1761.

Van Hooff T, Blocken B (2010). Coupled urban wind flow and indoor natural ventilation modelling on a high-resolution grid: A case study for the Amsterdam ArenA stadium. *Environmental Modelling & Software*, **25**(1), 51–65.